Observations of Extrasolar Planets During the non-Cryogenic Spitzer Space Telescope Mission

Drake Deming[*], Eric Agol[†], David Charbonneau[**], Nicolas Cowan[†], Heather Knutson[**] and Massimo Marengo[‡]

[*]*NASA's Goddard Space Flight Center, Planetary Systems Laboratory, Code 693, Greenbelt, MD 20771*
[†]*Department of Astronomy, University of Washington, Box 351580, Seattle, WA 98195-1580*
[**]*Department of Astronomy, Harvard University, 60 Garden St., MS-16, Cambridge, MA 02138*
[‡]*Harvard-Smithsonian Center for Astrophysics, 60 Garden St., MS-45, Cambridge, MA 02138*

Abstract. Precision infrared photometry from Spitzer has enabled the first direct studies of extrasolar planet physical properties, via observations at secondary eclipse in transiting systems. Current Spitzer results include the first longitudinal temperature map of an extrasolar planet, and the first spectra of their atmospheres. Spitzer has also measured a temperature and precise radius for the first transiting Neptune-sized exoplanet, and is beginning to make precise transit timing measurements to infer the existence of unseen low mass planets. The lack of stellar limb darkening in the infrared facilitates precise radius measurements of transiting planets. Warm Spitzer will be capable of a precise radius measurement for Earth-sized planets transiting nearby M-dwarfs, thereby constraining their bulk composition. It will continue to measure thermal emission at secondary eclipse for transiting hot Jupiters, and be able to distinguish between planets having broad band emission *vs*. absorption spectra. It will also be able to measure the orbital phase variation of thermal emission for close-in planets, even non-transiting planets, and these measurements will be of special interest for planets in eccentric orbits. Warm Spitzer will be a significant complement to Kepler, particularly as regards transit timing in the Kepler field. In addition to studying close-in planets, Warm Spitzer will have significant application in sensitive imaging searches for young planets at relatively large angular separations from their parent stars.

Keywords: keywords
PACS: PACS Info

INTRODUCTION

The Spitzer Space Telescope (Werner et al. [1]) was the first facility to detect photons from known extrasolar planets (Charbonneau et al. [2], Deming et al. [3]), inaugurating the current era wherein planets orbiting other stars are being studied directly. Cryogenic Spitzer has been a powerful facility for exoplanet characterization, using all three of its instruments. Spitzer studies have produced the first temperature map of an extrasolar planet (Knutson et al. [4]), and the first spectra of their atmospheres (Grillmair et al. [5], Richardson et al. [6]). Spitzer will continue to study exoplanets when its store of cryogen is exhausted. 'Warm Spitzer' (commencing $\sim$ spring 2009) will remain at T $\sim$ 35K (passively cooled by radiation), allowing imaging photometry at 3.6 and 4.5 μm, at full sensitivity. The long observing times that are projected for the warm mission will facilitate several pioneering exoplanet studies not contemplated for the cryogenic mission.

EXTRASOLAR PLANETS IN 2009

Currently over 200 extrasolar planets are known, including 22 transiting planets (17 orbiting stars brighter than V=13). Some of these have been discovered by the Doppler surveys, but an increasing majority of the transiting systems are being discovered by ground-based photometric surveys. However, the Doppler surveys remain an efficient method to find hot Jupiters, and surveys such as N2K (Fischer et al. [7]) continue to be a productive source of both transiting and non-transiting close-in exoplanets. The discovery rate from the photometric surveys is accelerating, because these teams have learned to efficiently identify and cull their transiting candidates, and quickly eliminate false positives. Several transit surveys (HAT, TrES, and XO) recently announced multiple new giant transiting systems (Burke et al. [8], O'Donovan et al. [9], Johns-Krull et al. [10], Mandushev et al. [11], Torres et al. [12]), and a Neptune-sized planet has been discovered transiting the M-dwarf GJ 436 (Gillon et al. [13]). We estimate that the number of bright (V<13) stars hosting transiting giant planets will increase to $\sim$100 in the Warm Spitzer time frame.

The discovery of transits in GJ 436b has stimulated interest in finding more M-dwarf planets, both by Doppler surveys (Butler et al. [14]), and using new transit surveys targeted at bright M-dwarfs. It is reasonable to expect that $\sim$10 transiting hot Neptunes will be discovered transiting bright M-dwarf stars by the advent of the warm mission. Moreover, the Doppler surveys are finding planets orbiting evolved stars (Johnson et al. [15]). The greater luminosity of evolved stars can potentially super-heat their close-in planets and facilitate follow-up by Warm Spitzer at 3.6 and 4.5 μm.

PHOTOMETRY USING WARM SPITZER

Warm Spitzer has a particularly important role in follow-up for bright transiting exoplanet systems, as well as non-transiting systems, because in 2009 it will be the largest aperture general-purpose telescope in heliocentric orbit. Heliocentric orbit provides a thermally stable environment, and it allows long periods of observation, not blocked by the Earth. Although Kepler will have a greater aperture than Spitzer, Kepler will be locked-in to a specific field in Cygnus, so it cannot follow-up on the numerous bright transiting systems that will be discovered across the sky.

The thermally stable environment of heliocentric orbit has proven to be a boon for precision photometry from Spitzer. For example, the recent Spitzer 8 μm observations of the HD 189733b transit reported by Knutson et al. [4], illustrated in Figure 1, are among the most precise transit observations ever made. These investigators measured the planet-to-star radius ratio for HD 189733b as 0.1545 ± 0.0002, corresponding to a precision of $\pm$ 90 km in the radius of the giant planet, and they also measured the orbital phase variation of the planet's thermal emission.

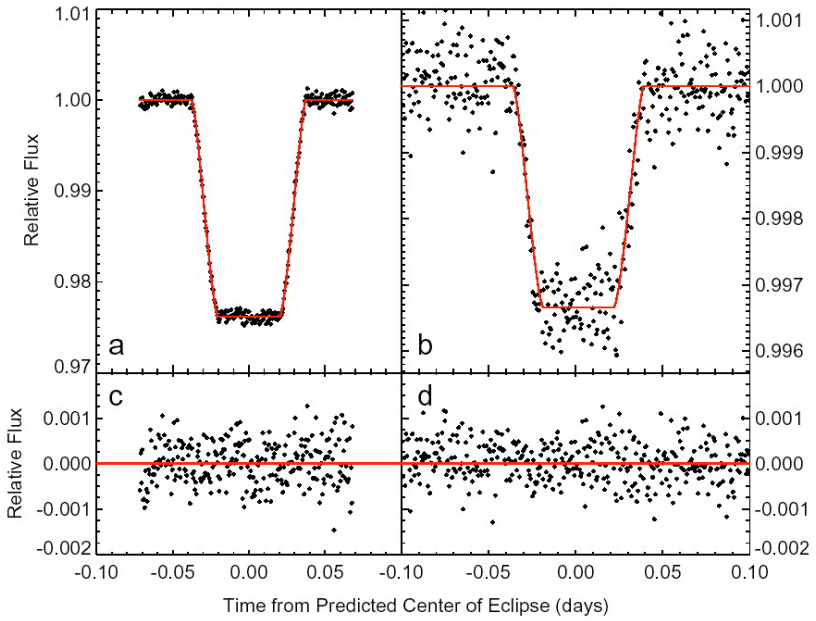

FIGURE 1. Transit (left) and a 60σ secondary eclipse detection (right) of HD 189733b at 8 μm using a continuous 30-hour Spitzer photometry sequence (Knutson et al. [4]).

MASS-RADIUS RELATIONS

Spitzer's precision for transits derives not only from its stable thermal environment, but also from the lack of stellar limb darkening in the IR. Without limb darkening, the transit becomes extremely 'box-like', with a flat bottom (Richardson et al. [24], Knutson et al. [4], see Figure 1). The IR transit depth yields the ratio of planet to stellar area simply and directly, without the added uncertainty of fitting to limb-darkening. Spitzer is now the facility of choice for transiting planet radius measurements. A Warm Spitzer transit program - exploiting the bright stellar flux at 3.6 and 4.5 μm - could significantly improve our knowledge of the mass-radius relationship, and clarify differences in bulk composition, for all but the faintest hot Jupiter systems. Figure 2 shows the mass-radius relation for several of the transiting giant planets (Charbonneau et al. [16]). The mass-radius relation encodes fundamental information on the global structure of these planets. For example, HD 149026b is inferred to have a heavy element core of at least 70 Earth masses, based on the small radius for its mass (Figure 2, and Sato et al. [25]). This information is crucial to our understanding of planet formation, e.g., by the core accretion and gravitational instability mechanisms (Lissauer & Stevenson [26]). The scientific utility of these measurements will be maximized if all transiting exoplanet radii are measured to high precision, in a mutually consistent manner. Moreover, as the Doppler and transit surveys discover Neptune to Earth-sized planets orbiting M-dwarfs, the highest precision photometry will be needed to measure their radii to a precision sufficient to constrain their interior structure.

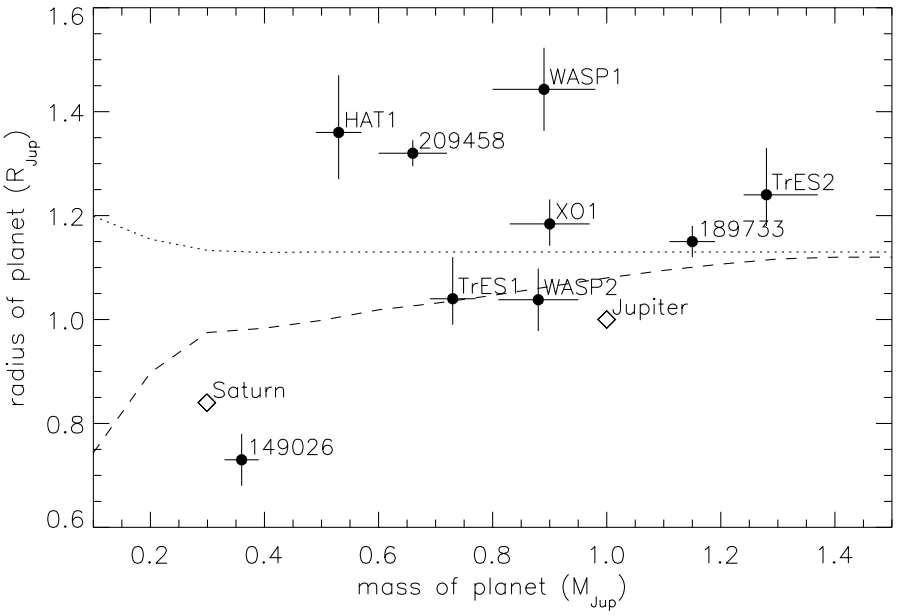

FIGURE 2. Mass-radius relation for giant transiting exoplanets, compared to Jupiter and Saturn (Charbonneau et al. [16]). The lines show the theoretical relations (Bodenheimer et al. [17] for planets having no core (dotted) and a 20 Earth-mass solid core (dashed).

Spitzer vs. Ground-Based Photometry

Ground-based photometry in the z-band is achieving sub-milli-magnitude levels of precision in many cases (Winn et al. [18]), and can determine the radii of some transiting giant planets to error limits imposed by astrophysical uncertainty in the stellar mass. The most favorable systems for ground-based observation are those occurring in fields with numerous nearby reference stars of comparable brightness. Planets transiting bright, spatially isolated, stars are not as favorable for ground observation. Moreover, as the radius of the transiting planet decreases, greater photometric precision is needed to reach the limits imposed by uncertainty in the stellar mass. Nearby M-dwarfs have flux peaks longward of the visible and z-band spectral regions, and they often lack nearby comparison stars of comparable infrared brightness. Neptune- to Earth-sized planets orbiting nearby M-dwarfs will therefore require infrared space-borne photometry for the best possible radius precision. Figure 3 illustrates a single transit of a 1-Earth radius planet across an M-dwarf, observed by Spitzer at 8 μm. We simulated this case by re-scaling a real case: Spitzer's recent photometry of GJ 436b (Deming et al. [19], Gillon et al. [20]). Spitzer's nearly photon-limited precision detects this Earth-sized planet to 7σ significance in a single transit.

Although Figure 3 is based on Spitzer observations at 8 μm, the photon-limit for observations during the warm mission (e.g., at 4.5 μm) will be even more favorable, simply because stars are brighter at the shorter wavelength. Stellar photometry at the wavelengths used by the warm mission is affected by a pixel phase effect in the IRAC

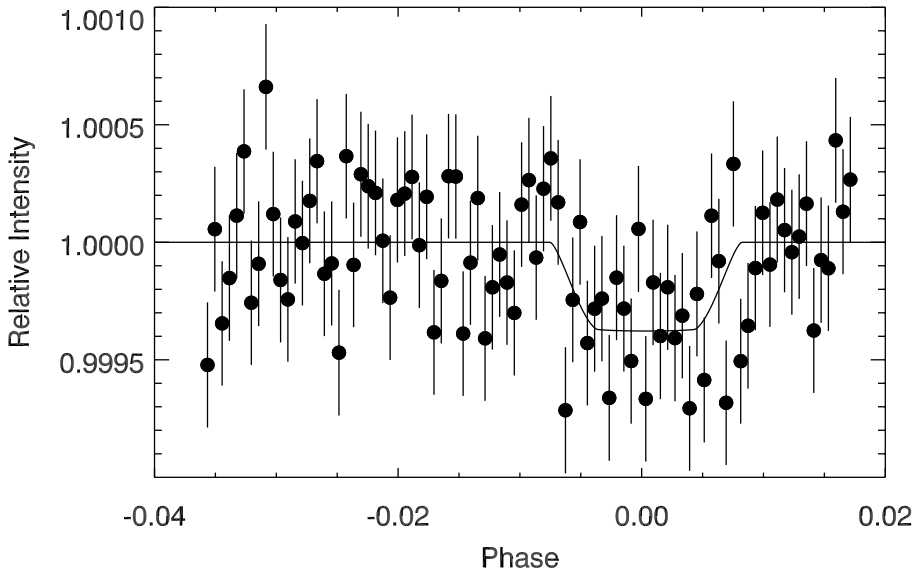

FIGURE 3. A transit of a 1 Earth radius planet across an M-dwarf, simulated by rescaling Spitzer 8 μm observations of GJ 436b (Deming et al. [19])

instrument (Reach et al. [21]), but that can be successfully corrected by decorrelation (Charbonneau et al. [2]), and recent results have demonstrated secondary eclipse detections with a precision of $\sim 10^{-4}$ (Charbonneau et al. [2], Knutson et al. [22]). The pixel phase effect should be correctable to even greater precison using the large data sets contemplated for the warm mission.

NEW TYPES OF TRANSITING PLANETS

Ongoing Doppler and transit monitoring of known hot Jupiters can detect subtle deviations from Keplerian orbits (Charbonneau et al. [27]), indicating the presence of additional planets, e.g., 'warm Jupiters' in longer period orbits, or terrestrial mass planets in low order mean motion resonances. The likely co-alignment of orbital planes increases the chance those planets will also transit, and intensive radial velocity monitoring could constrain the transit time for giant planets. Warm Spitzer will be a sensitive facility for confirming those transits, and extending the mass-radius relation (Figure 2) to planets in more distant orbits, and even to close-in terrestrial planets. Even lacking specific indications from Doppler measurements, searches for close-in terrestrial planets in low order mean motion resonances with known giant transiting planets (Thommes [29]) are warranted using Warm Spitzer. These searches could be combined with radius and transit timing measurements for the giant planets, in the same observing program.

For stars not known to host a hot Jupiter, ongoing Doppler surveys and space-borne transit surveys (e.g., COROT) will find more transiting planets, extending to Neptune

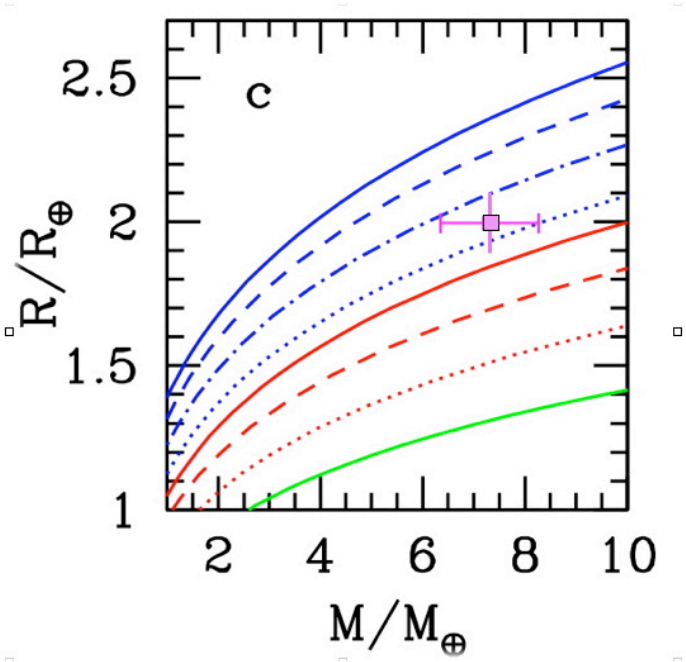

FIGURE 4. Mass-radius relations for solid exoplanets of various compositions, from Seager et al. [30]. Blue represents water ice planets, red are silicate planets, and green is a pure iron planet. The magenta point is a hypothetical observation of a hot Earth transiting an M-dwarf at 50 pc, observed by Warm Spitzer at 4.5 μm. The horizontal error bar is the mass error from Gliese 876d (Rivera et al. [28]); the vertical (radius) error bar is calculated for Warm Spitzer, not including error in the stellar radius.

mass and below. Spitzer transit measurements can precisely determine the radii of small planets. Exoplanet radius measurements and transit searches are particularly appropriate for Warm Spitzer, because: a) stars are bright in the 3.6 and 4.5 μm bands, while limb darkening is still absent, b) stellar activity is muted at IR wavelengths, and c) longer observing times are congruent with the aims of the extended mission. Figure 4 shows a potential example of a precise radius (allowing precise density) determination for a hot super-Earth, compared to the mass-radius relation for solid exoplanets of various composition (Seager et al. [30]). In this case, the Spitzer radius is sufficiently precise ($\pm$ 0.1 Earth radii) to constrain the bulk composition of this solid exoplanet by comparison to the Seager et al. [30] models.

THERMAL EMISSION AT 3.6 AND 4.5 μM

Absoption vs. Emission Spectra

Although the secondary eclipse of a transiting planet presents the largest signal at the longest wavelengths, the eclipses remain detectable at Spitzer's shortest wavelengths. Secondary eclipse photometry using Warm Spitzer can continue to define the brightness of exoplanets at 3.6 and 4.5 μm for new bright transiting systems. This will be especially

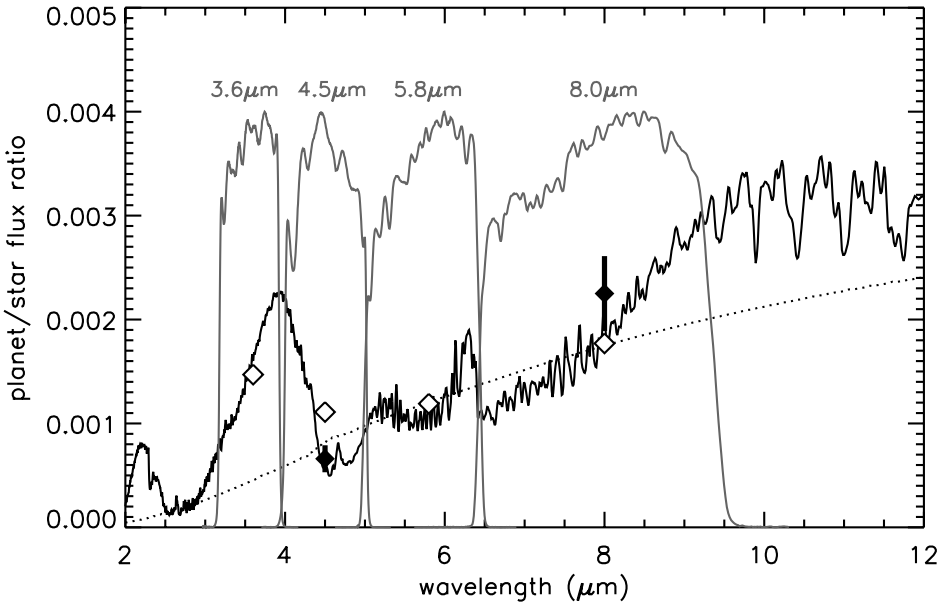

FIGURE 5. Predicted specturm of a hot Jupiter exoplanet, shown in comparison to observations of TrES-1 by Charbonneau et al. [2] (solid diamonds). The expected contrast (planet divided by star) for the IRAC bands is shown by open diamonds. Note the higher contrast expected at 3.6 μm compared to 4.5 μm, indicative of a water absorption spectrum. These contrast values will be reversed for a water emission spectrum. The dotted line is a blackbody spectrum.

valuable if complemented by ground-based detections exactly at the expected spectral peaks at 2.2 and 3.8 μm, which is believed to be feasible (Snellen and Covino [31], Deming et al. [32]). The predicted spectrum of a hot Jupiter exoplanet is illustrated in Figure 5, from Charbonneau et al. [2]. Normally, the broad band spectrum is expected to be shaped by water vapor absorption. However, recent Spitzer photometry of HD 209458b (Knutson et al. [22]) indicates much better agreement with a spectrum wherein the water bands appear in *emission*, due to a perturbed temperature structure (Burrows et al. [23]). This large departure from the predicted spectrum raises many fundamental questions concerning exoplanet atmospheric structure, whose investigation will be facilitated by observing many additional planets. Since the water bands have a particularly strong effect at Spitzer's shortest wavelengths, observations during the warm mission can readily identify those planets exhibiting emission spectra. Specifically, the relative contrast level in the 3.6 and 4.5 μm bands (diamonds on Figure 5) will be reversed for an emission spectrum. A survey of transiting hot Jupiters using 3.6 and 4.5 μm secondary eclipse photometry will be very valuable in selecting the most interesting planets for detailed spectroscopic follow-up using JWST. Moreover, because the Planck function is a strong function of temperature at shorter wavelengths, eclipse depths and phase curves (Cowan, Agol & Charbonneau [33]) for the hottest close-in planets at the warm mission wavelengths could also be a valuable means of monitoring exoplanet dynamics and variability over long times (Rauscher et al. [34]).

Time-Dependent Heating in Eccentric orbits

Extrasolar planets have more eccentric orbits on average than do the planets of our own solar system. In some cases, their eccentricity extends to strikingly high values. For example, HD 80606b has an eccentricity of 0.93 (Naef et al. [35]). During its close periastron passage, it receives a stellar flux more than 1000 times greater than the flux received by Earth from the Sun. This strong flux will cause a rapid heating of the planet's atmosphere, and its time dependence encodes crucial information on the radiative time scale, and thus the composition, of the planet's atmosphere (Langton and Laughlin [36]). This rapid heating of HD 80606b and similar systems may be observable at 3.6 and 4.5 μm. In this regard it is interesting to note that the exoplanet HD 185269b orbits a sub-giant star, having greater than solar luminosity, in a close orbit (6.8 day period), with an eccentricity of 0.3 (Johnson et al. [37]). The resultant strong variation in stellar heating over the orbit will force a corresponding variation in the planet's thermal emission, that should correlate with orbital phase. Recently, the transiting planets XO-3 and HAT-P-3 have also been found to have a significant eccentricity (Johns-Krull et al. [10], Torres et al. [12]), opening the possibility to also measure the spatial distribution of time dependent heating on the planet's disk (Williams et al. [38], Knutson et al. [4]). Given the high precision possible from Spitzer, it may be possible to observe all of these effects at 4.5 μm using Warm Spitzer.

TRANSIT TIMING

There is considerable recent interest in the indirect detection of extrasolar terrestrial planets via their perturbations to the transit times of giant transiting planets (Agol et al. [39], Holman and Murray [40], Steffen and Agol [41], Agol & Steffen [42]). Spitzer transit photometry during the warm mission is an excellent way to make precise transit timing measurements. The lack of IR limb darkening is again a significant advantage, because it results in very steep ingress and egress curves, producing the best possible timing precision. Also, the lower contrast of star spots and plage in the IR as compared to visible wavelengths minimizes stellar activity noise. Spitzer's heliocentric orbit permits continuous measurements before, during, and after transit - unlike Hubble where blocking by Earth interrupts transits. This potential was realized by Knutson et al. [4], who found a timing precision for the transit of 6 seconds. This is the most precise transit time ever measured: Hubble transit timing errors range from 10 to 50 seconds (Agol & Steffen [42]). Spitzer transit timing precision should be even better at the shorter wavelengths available for the warm mission, because stars are brighter at shorter wavelengths, and limb darkening remains negligible.

The continued success of the ground-based transit surveys, the advent of COROT, and the upcoming launch of Kepler, will provide a wealth of targets for Warm Spitzer follow-up. We have calculated the transit timing precision by Warm Spitzer at 3.6 and 4.5 μm, for solar-type stars at different distances (Figure 6). This calculation is consistent with the Knutson et al. [4] result, and it projects a Spitzer timing precision of better than 40 seconds down to the faint end of Kepler's range at V=14. This is sufficient to detect perturbations by terrestrial planets well below one Earth mass in resonant orbits (Agol et

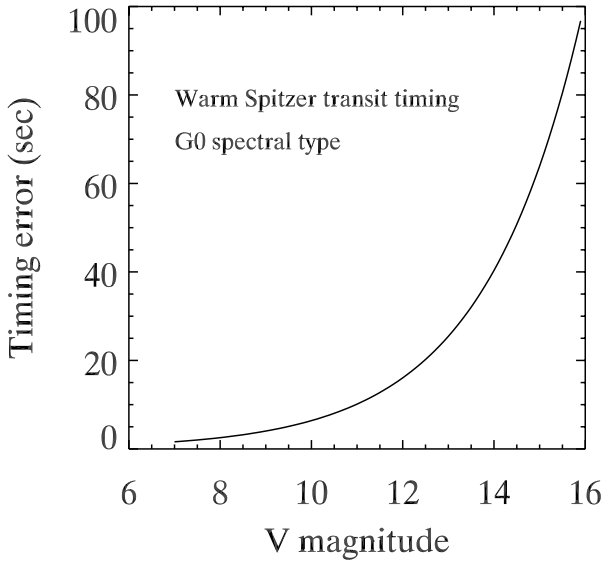

FIGURE 6. Calculation of the transit timing error (1σ) for Warm Spitzer observing giant planet transits at 4.5 μm, as a function of stellar brightness.

al. 2005), or to ~ 10 (150 days/P_1) Earth masses for $P_2/P_1 < 4$, where $P_{1,2}$ are the periods of the transiting and perturbing planets (Holman and Murray [40], Agol et al. [39]). The Warm Spitzer mission will begin at about the same time that Kepler begins to discover multiple new giant transiting planets (February 2009 launch). The observing cadence of the Kepler mission is not optimized for transit timing (Basri et al. [43]), so transit timing observations in the Kepler field by Warm Spitzer could leverage and enhance Kepler's science return.

DIRECT IMAGING

Although the bulk of Spitzer's results for exoplanets have relied on time series photometry and spectroscopy, Spitzer's high sensitivity in imaging mode is also important for exoplanet imaging studies. Radial velocity surveys have reached the precision required to detect planets only in the last 10 years, so little is known about the frequency of exoplanets and other low mass companions at distances greater than $\sim$ 5 - 10 AU. This is unfortunate because determining the presence of planetary mass bodies in the periphery of known exoplanetary systems has important implications for their evolution. These include studying the dynamical "heating" of the orbits in the system, which may result in higher eccentricities (or even expulsion) of some components, or in enhanced collision rates between the bodies in extrasolar Kuiper belts, which may be responsible for the formation of transient debris disks.

Imaging can in principle fill this observational gap. Three objects of near planetary

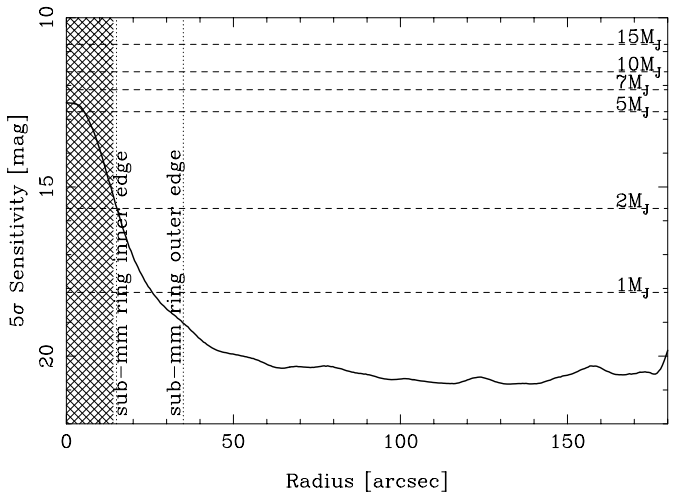

FIGURE 7. Residual noise, after PSF subtraction, of 4.5 μm ε Eridani radial profile (Marengo et al. [49]). Dashed lines are the predicted fluxes (from Burrows, Sudarsky, & Lunine [47]) of 1 Gyr old planets with mass from 1 to 15 M_J. Dotted lines enclose the region where the sub-millimeter debris disk around this star is located.

mass have already been detected within 300 AU from the primary around the brown dwarf 2M1207 (Chauvin et al. [44]) and the stars GQ Lup (Neuhauser et al. [45]) and AB Pic (Chauvin et al. [46]) with ground based adaptive optics observations. Other optical and near-IR searches from the ground and from space, have so far produced negative results.

Warm Spitzer may provide a significant contribution in this arena, as the two surviving IRAC bands are particularly suited for the detection of cool extrasolar planets and brown dwarf companions (T and the so-called Y dwarfs). A gap in molecular opacities of giant planets near 4.5 μm allows emission from deep, warmer atmospheric layers to escape: giant planets are very bright at this wavelength (Burrows, Sudarsky, & Lunine [47]). A strong methane absorption band strongly depresses the planetary flux at 3.6 μm: as a result, the IRAC [3.6]-[4.5] color of planetary mass bodies is expected to be unique, and allow for their identification among background objects in the field. Model atmosphere calculations predict that a 1 Gyr old, 2 M_J planet around a star 10 pc from the Sun will have a 4.5 μm magnitude of $\sim$ 18. Such planets are detectable today with IRAC provided that the diffracted light from the central bright star can be removed at the planet's image location. The stability of Spitzer's optical and pointing systems assures that the stellar Point Spread Function (PSF) is highly reproducible, allowing much fainter nearby sources to be identified in the PSF wings using differential measurements.

This search has already been carried out for the debris disk star ε Eridani, which is also home of a Jovian class radial velocity planet orbiting the star at 3.4 AU (Hatzes et al. 2000). The search has set stringent limits for the mass of external planetary bodies in the system (including the area occupied by the debris disk, Marengo et al. [49]), and demonstrated that this technique is sensitive to the detection of planets with mass as low as 1 M_J (Figure 7) outside the 14 arcsec radius (50 AU) where the IRAC frames are saturated. The search radius can be reduced to $\sim$ 5 arcsec or less by using shorter frame

times available in IRAC subarray mode. A pilot search of 16 nearby stellar systems is being conducted in Spitzer cycles 3 and 4. These programs will identify possible candidates based on their [3.6]-[4.5] colors, which will need to be verified by second epoch observations during the warm mission, to detect their common proper motion with the primary.

The Spitzer warm mission will provide the opportunity to extend the search of planetary mass companions through imaging techniques to a large number of systems in the solar neighborhood, probing a search radius from $\sim$ 10 to 10,000 AU around stars within 30 pc from the Sun. This search will be sensitive to masses as low as a few Jupiter masses, depending on the age and distance of the systems. These observations will be complementary to ground based radial velocity and imaging searches with adaptive optics systems, given the larger field of view and higher sensitivity of IRAC, in a wavelength range where the required contrast ratio (as low as 10^{-5} of the parent star flux) is more accessible than in the optical and near-IR.

ACKNOWLEDGMENTS

We thank the Spitzer Science Center for the opportunity to consider and discuss the potential for exoplanet science during the warm mission. We are grateful to Josh Winn and Andy Gould for helpful conversations and remarks regarding the relative merits of of ground-based vs. space-borne photometry. We also acknowledge informative conversations with Greg Laughlin on the effects of heating in eccentric orbits.

REFERENCES

1. Werner, M. W., et al., 2004, ApJS, 154, 1.
2. Charbonneau, D., et al. 2005, ApJ, 626, 523.
3. Deming, D. et al., 2005, Nature, 434, 740.
4. Knutson, H., et al., 2007a, Nature, 447, 183.
5. Grillmair, C. et al., 2007, ApJ 658, L115.
6. Richardson, L. J. et al., 2007, Nature 445, 892.
7. Fischer, D., et al. 2005, ApJ 620, 481.
8. Burke, C., et al. 2007, submitted to ApJ, (astro-ph/0705.0003).
9. O'Donovan, F. T., et al. 2007, ApJ 663, L37.
10. Johns-Krull, C., et al. 2007, BAAS 39, 096.05.
11. Mandushev, G., et al. 2007, ApJ, in press, (astro-ph/0708.0834).
12. Torres, G., et al. 2007, ApJ, 666, L121.
13. Gillon, M., et al. 2007a, A&A, 472, L13.
14. Butler, R. P., et al., 2004, ApJ 617, 580.
15. Johnson, J. A., et al. 2007, ApJ, in press (astro-ph/0704.2455).
16. Charbonneau, D., et al. 2006, ApJ 636, 445.
17. Bodenheimer, P., Laughlin, G., and Lin, D. N. C. 2003, ApJ 592, 555.
18. Winn, J. N., et al., 2007, AJ 133, 1828.
19. Deming, D., et al., 2007a, ApJL, in press, (astro-ph/0707.2778).
20. Gillon, M., et al., 2007b, A&A 471, L51.
21. Reach, W. T., et al., 2005, PASP 117, 978.
22. Knutson, H., et al., ApJ, submitted.
23. Burrows, A. et al., ApJL, in press.
24. Richardson, L. J. et al., 2006, ApJ 649, 1043.

25. Sato, B., et al. 2005, ApJ 633, 465.
26. Lissauer, J. J. and Stevenson, D. J., 2007, in Protostars and Planets V, (eds. D. Jewitt and B. Reipurth), 591.
27. Charbonneau, D., et al. 2007, in Protostars and Planets V, (eds. D. Jewitt and B. Reipurth), 701.
28. Rivera, E. J., et al., 2005, ApJ 634, 625.
29. Thommes, E. W., 2005, ApJ 626, 1033.
30. Seager, S., et al., 2007, ApJ, in press (astro-ph/0707.2895).
31. Snellen, I. A. G., and Covino, E., 2006, MNRAS 375, 307.
32. Deming, D. et al., 2007, MNRAS, 378, 148.
33. Cowan, N. B., Agol, E., & Charbonneau, D., 2007, MNRAS, 379, 641.
34. Rauscher, E., et al. 2007, ApJ, 662, L115.
35. Naef, D., et al., 2001, A&A 375, L27.
36. Langton, J., and Laughlin, G., 2007, ApJ 657, L113.
37. Johnson, J. A., et al. 2006, ApJ 652, 1724.
38. Williams, P. K. G., et al., 2006 ApJ 649, 1020.
39. Agol, E., et al., 2005, MNRAS 359, 567.
40. Holman, M. J., and Murray, N. M., 2005, Science 307, 1288.
41. Steffen, J., and Agol, E., 2005, MNRAS 364, L96.
42. Agol, E., and Steffen, J., 2007, MNRAS 374, 941.
43. Basri, G., Borucki, W. J., and Koch, D. 2005, New Astron. Rev. 49, 478.
44. Chauvin, G. et al., 2004, A&A 425, L29.
45. Neuhauser, R. et al. 2005, A&A 345, L13.
46. Chauvin, G. et al., 2005, A&A 438, L29.
47. Burrows, A., Sudarsky, D., & Lunine, J. L. 2003, ApJ 596, 587.
48. Hatzes, A. P. et al., 2000, ApJ 544, L145.
49. Marengo, M. et al., 2006, ApJ 647, 1437.